Renewable Energy
June 2014, Volume 66, Pages 670–679
http://dx.doi.org/10.1016/j.renene.2014.01.012

Spatial and temporal characteristics of wind and wind power off the coasts of Brittany

Abderrahim Bentamy*, Denis Croize-Fillon

Laboratoire d'Océanographie Spatiale, IFREMER, France

*: Corresponding author : Abderrahim Bentamy, email address : abderrahim.bentamy@ifremer.fr

Abstract:

The main objective of this paper is to thoroughly examine the remotely sensed wind characteristics around the coasts of Brittany as well as some more specific areas. The offshore wind power potential is then assessed. To achieve this objective, information on wind speed and direction with sufficient spatial and temporal sampling under all weather conditions and during day and night is required. This study uses more than 12 years (December 1999–December 2012) of consistent remotely sensed data retrieved from the ASCAT and QuikSCAT scatterometers to estimate the conventional moments and associated wind distribution parameters. The latter are comparable to wind observations from meteorological stations. Furthermore, combining in-situ and scatterometer wind information enables an improved assessment of the spatial and temporal wind structures at specific locations of interest to be made. The wind statistical results are used to study the spatial and temporal patterns of the wind power. Although the main parameters characterizing wind power potential such as mean, variability, maximum energy, wind speed and intra-annual exhibit seasonal features, significant inter-annual variability is also depicted. Furthermore, differences are found between the wind power estimated for northern and for southern Brittany.

Highlights

► Using scatterometer retrievals for MRE purposes. ► Spatial and temporal structures of wind off Brittany coasts. ► Spatial and temporal characteristics of wind energy.

Keywords: Wind ; Energy ; Scatterometer ; Remote sensing ; Brittany

1. Introduction

Several countries have set up ambitious programmes aiming to investigate the capability of renewable marine energy operational productions. In France, the “Grenelle de la Mer” (http://www.legrenelle-environnement.fr/) suggests that marine energy derived from various platforms and sources would provide 3% of the total required energy and could reach a production level of 6000 MW in 2020. Such an objective requires precise knowledge of the parameters characterizing the oceanographic and atmospheric parameters at various spatial and temporal scales. In particular, it means the acquisition and analysis of a significant sample of the resource of primary interest, such as wind (speed and direction), waves (significant heights, directions, peaks, and spectra), currents and stratification (depth of the mixed layer). Precise knowledge of these parameters with high accuracy and spatial and temporal resolution is necessary for the proper design of structures and to estimate the environmental risks.

Among the sources of marine renewable energy (MRE), wind energy exploitation is growing fast. Even though wind farm installations are still costly, their developments meet the public awareness about environmental issues, and the energy produced would contribute to the regional energy supply and security. The project called "France Energies Marines" (http://www.france-energies-marines.org/) is one the main programmes aiming to assess wind resource requirements. Some experimental sites located off the coasts of France have been selected to achieve this. Here, the areas of interest are located offshore of Brittany in the north-west of France (Figure 1). These areas are characterized by one of the most important wind energy resources in France. The dominant winds over this region are westerly winds. Furthermore, high winds reaching 50-60m/s can occur during the winter season due to westerly storms.

In this study, wind resources are mainly derived from scatterometers which provide surface wind vector information over the global oceans. Various attempts regarding the evaluation of wind energy potential for different oceanic areas based on remotely sensed data have been carried out (e.g. [1], [2], [3]). To our best knowledge, there are no previous publications focusing on the analysis of wind energy potential for the coasts of Brittany based on scatterometer retrievals. Various scatterometers can be used to assess the wind resources, such as ERS-1 (1991 – 1996), ERS-2(1995 – 2011), NSCAT (1996-1997), Seawinds onboard QuikSCAT (1999 – 2009), Seawinds on board ADEOS-2 (2003), ASCAT onboard METOP-A (2006 – Present). Here, only retrievals from QuikSCAT and from ASCAT are used. Both winds compare well, and their consistency has been established in recent work [4]. Remotely-sensed wind data with a high spatial resolution of 12.5km×12.5km are available. Furthermore, coastal winds are also retrieved from ASCAT measurements.

Here, the distribution of wind resources between the near-shore and offshore regions around Brittany are evaluated using twelve years of remotely-sensed data (December 1999 – December 2012). Such a long time series is extremely valuable to assess the wind regimes and wind energy related quantities over extended oceanic areas. It is also helpful to highlight the most appropriate locations for energy production and thus for wind turbine installation.

The paper contents are as follows: in section 2 the data used, the quality checks, and the required wind corrections used in the study are described. Section 3 deals with the comparisons between in-situ and remotely-sensed winds. The analyses of the distribution of wind and the related wind power are presented in sections 4 and 5, respectively. The conclusions are listed in section 6.

2. DATA

2.1. Remotely sensed data

The scatterometer principle is described in many scientific publications. Scatterometer antennae emit microwaves towards the surface, which are scattered by short sea waves (capillary/gravity waves). The latter are strongly related to changes in surface winds. Surface wind speeds and directions are available over scatterometer swaths with various orbit and spatial resolution characteristics. This study relies on winds retrieved from SeaWinds scatterometer onboard QuikSCAT satellite, and from Advanced Scatterometer (ASCAT) onboard Metop-A satellite. Readers may found complete descriptions of the two scatterometers and of the associated retrievals in [9] for QuikSCAT, and on the SAF OSI website http://www.knmi.nl/scatterometer/ for ASCAT. They provide valuable information related to instrument physics, retrieval and ambiguity removal methods, rain detection and flagging techniques, and quality control procedures. Briefly, QuikSCAT is a rotating antenna with two differently polarized emitters: the H-pol with incidence angle of 46.25° and V-pol with incidence angle of 54°. The inner beam has a swath width of about 1400km, while the outer beam swath is 1800km width. The QuikSCAT scatterometer is a Ku band radar, therefore rain has a substantial influence on its measurements. Previous studies showed that the rain impact may attenuate the scatterometer signal resulting in wind speed underestimation, or raindrop impacts may change the sea surface shape resulting in overestimation of the retrieved winds. Results from [5] indicate that rain backscatter contributes to the scatterometer signal resulting generally in wind speed overestimation; intense rain causes overestimates of 15-20 m/s for cross-track winds. So, rain attenuation dominates over rain backscatter for extreme winds. QuikSCAT wind products include several rain flags determined from the scatterometer observations and from the collocated radiometer rain rate onboard other satellites. This study uses new QuikSCAT wind retrievals called QuikSCAT *V3* (ftp://podaac.jpl.nasa.gov/OceanWinds/quikscat/preview/L2B12/v3/). They are made available by Jet Propulsion Laboratory (JPL)/ Physical Oceanography Distributed Active Archive Center (PODAAC) scientific team [6]. QuikSCAT *V3* products are calculated through use of a geophysical model function ensuring the consistency with winds retrieved from microwave radiometers such as Special Sensor Microwave/Imager (SSM/I) and WindSat [7].QuikSCAT wind retrievals are provided over swaths at a Wind Vector Cell (WVC) of 12.5km spatial resolution. This new scatterometer product is assumed to improve wind speed performance in rain and at high wind speed conditions.

ASCAT has an engineering design that is quite different from QuikSCAT. Rather than a rotating antenna it has a three beam antenna looking 45° (fore-beam), 90° (mid-beam), 135° (aft-beam) of the satellite track, which together sweep out two 550 km swaths on both sides of the track. The incidence angle varies in the range 34°-64° for the outermost beams and 25°-53° for the mid-beam, giving Bragg wavelengths of 3.2-5.1cm and 3.6-6.8 cm. Here we use three types of ASCAT products: level 2b ASCAT near real time at 25x25 km^2 resolution, level 2b125 product available with higher spatial resolution of 0.125°x0.125° along and cross swath, and the product providing coastal information, referred to as the ASCAT coastal product, which is available with a resolution of 0.125°x0.125°. The products are available from Eumetsat Ocean Sea Ice Satellite Application Facility (OSI/SAF) (http://www.osi-saf.org/). Details of calibration, validation, and processing schemes can be found at (http://www.knmi.nl/scatterometer/). Hereafter, the three ASCAT wind products are referenced as ASCAT25 (available from April 2007 through to present), ASCAT125 (February 2009 – present), and ASCAT_coast (August 2010 – present), respectively. Comparisons to independent mooring and shipboard observations by [8] and [9] show that ASCAT25 wind speed and direction have rms difference values (in-situ minus scatterometer) of about 1.40m/s, and 18°, respectively. A similar validation procedure has been applied to ASCAT125 and ASCAT_coast to assess the quality of wind speed and direction retrievals [10]. The findings indicate that ASCAT high resolution products have accuracy similar to the low resolution data. For instance the rms differences (buoy minus scatterometer winds) of zonal as well as meridional components are about 1.50m/s.

The accuracy of the QuikSCAT *V3* data is determined through various comparisons with buoy wind measurements, QuikSCAT *V2*, and ASCAT retrievals. The main findings (not shown) are the comparison results are similar to those obtained previously (e.g. [4]). QuikSCAT *V3* and QuikSCAT *V2* exhibit similar comparison results versus buoys. ASCAT and QuikSCAT *V3* statistics are of the same order as ASCAT and QuikSCAT *V2*. Similar agreements and discrepancies characterizing ASCAT and QuikSCAT *V2* comparisons are found for ASCAT and QuikSCAT *V3*. QuikSCAT *V3* are improved when compared with the earlier results reported by [4]. We expect that the remaining discrepancies between the C-band radar and the Ku-band radar wind retrievals are inherent in their characteristics, such as the penetrating wavelengths of the radars and differences in the backscatter from surface waves at different wavelengths. Such effects would be pronounced in low wind speed regimes and at certain values of SST.

Wind speeds derived from ASCAT and from QuikSCAT are corrected with respect to results which assessed the coherency between C-and and Ku-band retrievals ([3], [11]). Briefly, only

QuikSCAT rain-free data associated with multidimensional rain probabilities ([12]) lower than 0.05 are selected. For ASCAT wind corrections, the bias dW (eq. (1)) was determined by fitting the mean difference between QuikSCAT and ASCAT winds as a function of ASCAT wind speed (W_{AS}) and azimuth direction (φ) ranges.

$$dW = \sum_{m=0}^{m=3} P_5^m (W_{AS}) \cos(m\phi) \ , \qquad (1)$$

Where the coefficients $P_5^m(W_{AS})$ are assumed to be fifth order polynomials of ASCAT wind speed.

Hereafter, ASCAT wind speed refers to W_{AS}+dW.

Figure 1 shows the spatial distribution of the sampling length of wind speed observations derived from scatterometers QuikSCAT and ASCAT during the period December 1999 through December 2012. It is shown at grids of 0.125 degree in longitude and latitude. ASCAT retrievals available with a swath spatial resolution of 0.25 degree are attributed to the closest 0.125° grid point. As expected, the highest and lowest observation numbers are found offshore and near-shore, respectively. Most of the data located 25km – 12.5km from coasts are derived from ASCAT coastal product.

2.2. In-situ data

To assess the wind statistics calculated from remotely-sensed wind retrievals along Brittany's coasts, anemometer 10-m wind measurements are used for comparison purposes (Figure 2). Indeed, they are assumed to capture fine-scale local winds that may be influenced by orography and local air-sea interaction impacts. Table 1 shows their WMO identification and their locations. They are land-based operational meteorological stations located near shores and managed by Météo-France (MF). Although the stations have been operating for several years, only winds measured during the period March 2008 through August 2012 are available for this study. Winds from stations are available at 10-m height and every 30 minutes, one hour or three hours depending on the station. Since scatterometers provide equivalent neutral winds (ENWs) at 10-m above the sea surface, in-situ winds should be corrected according to the atmospheric stability. This correction is performed using COARE3.0 model [13].

The entire station dataset are checked for erroneous values. Values of about 0m/s or exceeding 50m/s are not considered in this study. The outliers of winds reported from each station are first detected based on the use of the daily averaged wind estimates. The latter are estimated every day as mean values of the consecutive raw data available from 00h:00 through 21h:00UTC every 3 hours. The daily variability is calculated as standard deviation values (STD). Each “raw” observation exceeding the daily mean value by a factor of three times the STD is removed as an outlier.

3. IN-SITU AND SCATTEROMETER WIND COMPARISONS

This study does not deal with the determination of the accuracy of scatterometer retrievals based on the use of station measurements. The main aim of the in-situ and scatterometer wind comparisons is to highlight the agreements and discrepancies between the two sources. The results are first used to support the comparisons between wind distributions determined from in-situ and from remotely-sensed data and to assess how scatterometer retrievals may represent near-shore surface winds.

3.1. Collocation procedure

Station and scatterometer wind comparisons require first the data to be collocated in space and time. Indeed, the spatial and temporal wind variability derived from in-situ and from remotely-sensed data may lead to significant differences. Therefore, the collocation criteria should be defined with respect to the time and space characteristics. They are estimated based on the method of Crosby et al. [14] dealing with the determination of spatial and temporal correlation coefficients:

$$\rho^2\,(X,\delta t) = \rho^2(Wst(X_0,0),Wsc(X,\delta t)) \quad (2)$$

$$\rho^2\,(X_0,\delta t) = \rho^2(Wst(X_0,0),Wst(X_0,\delta t)) \quad (3)$$

Where ρ^2 is the correlation coefficient between two vectors (time series). Wst and Wsc indicate wind speed from stations and from scatterometers, respectively. $Wst(X_0,\delta t)$ and $Wsc(X,\delta t)$ are wind speed time series at location X(x,y) shifted δt hours from stations and from scatterometers, respectively. X_0 states for station location. Equation (2) leads to the characterization of the spatial and temporal structures, whereas equation (3) estimates the temporal cross-correlation of station time series.

For lag time, δt, of one hour, $\rho^2\,(X_0,\delta t)$, estimated for each in-situ wind speed time series, varies between 0.86 and 0.90. The highest time correlations are found at Ouessant (07100) and Penmarc’h (07200) both stations being the most exposed to prevailing winds (Figure 2). Increasing the lag time to two or three hours leads to a decrease in the correlation variation by a factor of about 6% and 14%, respectively. For instance, for δt of 2 hours, only correlations $\rho^2\,(X,\delta t)$ (eq. 3) estimated at Ile de Groix (07203), Ouessant (07100), and Pointe du Raz (07103) exceed a threshold of 0.80. Selecting a lag time of less than 1 hour, the spatial correlation between each station and remotely sensed data (Wst and Wsc (eq. (2))), calculated as a function of spatial separation (distance between X_0 and X), are shown in Figure 3. It indicates that spatial correlation values are lower than 0.80 for distances exceeding 100km. At stations Ile de Batz (07116), and Saint Nazaire (07216) correlations do not reach 0.80 even for shorter distances. Ile de Batz is a land station located about 600 meters inland. Saint Nazaire is located in relatively narrow inlets compared to the scatterometer WVC spatial resolution (about 25km² or 12.5km²). The spatial correlations found for distances lower than 25km at Ouessant (07100), Penmarc’h (07200), and Pointe du Raz (07103) are of the same order as the temporal correlation ρ^2 (X_0,δt) calculated for one hour time lag. Further investigations are performed to assess the spatial and temporal correlations according to wind direction sectors. For a time lag of 1 hour, the highest spatial correlations are found for westerly winds (most prevailing regional wind condition) at all stations, except at Ile de Batz (07116). Indeed, their values exceed 0.80 and reach 0.95 for spatial distances ranging between 12.5km and 100km. Better spatial correlation results are obtained at Ile de Batz for easterlies. Only correlations estimated at Ouessant have values exceeding 0.80 for all sectors and for separations less than 100km.

For this study only spatial and temporal separations leading to correlations exceeding 0.80 are retained. Indeed, the threshold 0.80 meets the correlation result characterizing the comparison between buoy, moored off European coasts, and scatterometer wind speeds (e.g [8]). Following this analysis of spatial and temporal correlations, stations 07116 and 07216 are excluded and the procedure aiming to collocate in-situ and scatterometer winds is performed based on the space and time criteria of 25km and 1 hour, respectively.

3.2. Comparison results

Figure 4 shows results illustrating the comparisons of meteorological station and ASCAT scatterometer wind speeds during the period 2008 - 2012. The latter are from ASCAT retrievals since they are available throughout 2008 – 2012 period. Similar results are obtained for station and QuikSCAT wind comparisons during their overlapping period (January 2008 – November 2009). Statistical parameters of scatterometer retrievals against station measurements are presented in Table 2. The results are provided for all collocated data (Figure 4a) as well as for collocated data at Ouessant station (Figure 4b), as the results found in the previous section (3.1) indicate that the best agreement between in-situ and scatterometer wind speeds is found at this specific station. Although the comparison for all collocated data (Figure 4a) indicates quite good agreement between the two sources, the scatterometer wind speeds tend to be overestimated with respect to in-situ measurements. The mean bias is about -0.80m/s and the associated standard deviation (STD) is about 2.20m/s. This overestimation is not found at Ouessant station (Figure 4b), however, where the bias and STD are 0.07m/s and 1.66m/s, respectively. The latter meet the statistical results aiming to characterize retrieval quality based on collocated moored buoy and scatterometer winds (e.g. [8]). Therefore, the larger departures found when all collocated data are selected are the result of expected differences between onshore and coastal wind speeds (e.g. [15]). The frequency of occurrence of calm and light winds tends to be larger at onshore than nearshore sites. For instance, the percentage of wind speeds lower than 5m/s are about 37% and 25% for in-situ and scatterometer winds, respectively. Only the station Pointe du Raz (07103) shows a higher mean wind speed than the scatterometer, which is the result of more high wind conditions. Indeed, the 90 and 95 percentiles are of 13m/s and 15m/s, respectively, whereas they do not exceed 11m/s and 13m/s for the rest of stations. Investigating station and scatterometer wind speeds as a function of wind direction sectors disclosed differences in statistical results. For instance, the best results (low bias and STD, and high correlation) are found for stations 07207, 07203, 07100, 07200 in the presence of westerlies. Further comparisons based on monthly-averaged wind speed time series calculated from collocated data also reveal that the seasonal features of scatterometer-derived retrievals match those of in-situ data. Both indicate that the maximum and minimum winds occur during the periods November – January and June-August, respectively.

4. SCATTEROMETER WIND DISTRIBUTIONS

The results provided in section above, based on analysis of time- and space-collocated data, indicate that remotely-sensed winds realistically represent local winds occurring off the coasts of Brittany. Here we focus on the determination of wind speed distributions using only scatterometer winds from the period December 1999 – December 2012.

4.1. Influence of scatterometer sampling scheme

One of the main issues is that the remotely-sensed data are only available from morning and afternoon passes: 4h-6h UTC and 17h-19h UTC for QuikSCAT; and 9h-11h UTC and 20h-22h UTC for ASCAT. Therefore, the impact of such temporal sampling schemes should be studied prior the determination of wind speed distribution from satellite observations. To achieve such objective, data from in-situ sations are used. At each station, statistical parameters such as the mean, median, STD, skewness (Skew), kurtosis (Kur), 10 (P_{10}), 90 (P_{90}), and 95 (P_{95}) percentiles are calculated based first on all valid data, and secondly on only data occurring within one hour of scatterometer overpasses (Table 3). The two calculations are shown for each station on the top and bottom row, respectively. Both show similar wind speed distributions at each in-situ location. Selection of station data associated with scatterometer overpasses shows wind distributions which are slightly positively biased with respect to the distributions estimated from the full dataset. However, the bias is small, about 0.10m/s. Furthermore, using the Student's t-distribution test, the two wind speed means estimated for stations Ile de Batz(07116), Ile de Groix(07203), Ouessant(07100), Pointe du Raz(07103), Saint Nazaire(07216) are comparable at the 95% confidence level.

4.2. Spatial wind distribution

Using ASCAT and QuikSCAT data lead to estimate accurate time means and variabilities of surface winds over the coastal and offshore regions around Brittany. Furthermore, as shown above, the results may be extended to some near shore locations. Seasonal mean wind speed and direction patterns, estimated from the two scatterometers for winter (December-January-February (DFJ)), spring (March-April-May (MAM)), summer (June-July-August (JJA)), and fall (September-October-November (SON)), over 12 years (December 1999 through December 2012) are shown in Figure 5. The seasonal spatial distributions (not shown) of sampling length (number of retrievals falling within a 0.125°×0.125° grid point during the study period) are similar to those shown in Figure 1. The lowest sampling length values are found during winter and fall, the result of eliminating rain impacted data (mainly from QuikSCAT). Overall, however, the seasonal variability of the sampling length is quite small. Indeed, on average for offshore (resp. near-shore) grid points the numbers of rain-free data are about 1670 (887) in winter and 1870 (968) in summer.

Wind speed and direction distributions (Figure 5) correspond to the usual wind patterns for the region, with westerly winds prevailing. The patterns are mainly associated to the prevailing atmospheric circulation characteristics over Northeast Atlantic Ocean. Offshore wind speeds along Brittany coasts exhibit pronounced seasonality, with winter wind speeds almost 50% higher than summer values. The mean wind speed values are about 9m/s and 5.50m/s in winter and summer seasons, respectively, over the region. Winter winds are characterized by larger vertical shear and smaller interstability shear differences whereas in summer, winds tend to be lower due a relaxed meridional temperature gradient and a predominantly stable surface layer. The highest winds are found around northern coasts, mainly due to the channeling effect of the English channel. The spatial variability tends to be low, which is expected from results provided above (section 3). The main spatial differences are found between winds occurring in the northern and southern zones of Brittany. The highest mean winds are found over north-western areas, with the lowest in the south-east. The time variation, which can be estimated as the STD of the seasonal wind speed time series at each grid point, is higher during winter and fall, reaching 4.5m/s offshore, whereas during the summer season, STD values do not exceed 3m/s. Similar STD values are found for nearshore grid points.

The spatial distributions of remotely-sensed wind directions lead to fairly steady patterns. On average, winds occurring offshore are mostly westerly in winter, north-westerly (NW) in spring in southern areas, and are south-westerly (SW) in northern, and NW in southern areas during summer and fall. However, such mean patterns should be treated with caution, as the time variability of seasonal zonal and meridional wind components are high. For instance, the STD of the zonal component varies between 5m/s and 8m/s and between 3m/s and 6m/s during winter and summer, respectively. To highlight the wind vector variability, the wind direction frequencies are determined for two zones located north and south of 48°N during winter and summer seasons (Figure 6). Wind directions are given in the oceanographic convention (wind blowing towards). Even though the westerlies (wind direction of 270°±30° versus north) are prevailing over the two regions and for the two seasons, they only account for about 14% and 11% of occurrences in the northern and southern regions during the winter season. The percentages are calculated with respect to the total number of data from the particular region and season. The corresponding easterlies account for about 7% and 8%, respectively. During the summer, the frequency of westerlies decreases to 11% in the northern area, whereas it increases to 16% in the southern zone. The easterlies drop to about 4% in the two regions during the summer. Figure 6 also shows that wind speed conditions are wind direction dependent, with the highest winds associated with westerlies and occurring particularly during winter. For instance, wind speeds in southern and northern areas are above 12m/s for about 5.7% and 4.2% of the time, respectively. The frequency drops to 1.7% and 1.2% for easterly wind conditions. Although the percentage of 10m winds higher than 20m/s is quite small (approximately 0.2% of total data), they number 14827 and 89% of such high winds are westerlies, occurring 93% of the time during winter or fall. Low winds (less than 5m/s) account for 22% of all winds, and their easterly and westerly distributions (Figure 6) are similar. The number of low winds reaches a minimum during the winter season for 12% of the time, and a maximum during summer for 36% of the time.

5. WIND POWER

Previous results allow the determination and analysis of wind power density only estimated from scatterometer retrievals. It aims to characterize the resource availability at local scales over Brittany region.

5.1. Determination Method

The distribution of the wind power density (E) over Brittany offshore zone is determined from available winds. It may be directly estimated from time series at each grid point, based on the following formulae:

$$E=\frac{1}{2}\rho\overline{W^3} \quad (4)$$

where ρ is the air density, assumed to be a constant 1.225kgm^{-3} (at 10°C), and W is wind speed.

Alternatively, E may be estimated based on the wind speed density probability function (pdf), using the following relationship:

$$E=\frac{1}{2}\rho A^3\Gamma\left(1+\frac{3}{C}\right) \quad (5)$$

where A and C are the parameters of the Weibull pdf [16] and Γ denotes the Gamma function.

The Weibull pdf of wind speed (W in m/s) is expressed as:

$$P(W; A, C) = (C/A)(W/A)^{C-1}exp(-(W/A)^{C}) \quad (6)$$

A is a scaling parameter expressed in m/s, and C is a dimensionless shape parameter.

P indicates the probability of wind speed occurrence.

Several methods exist to estimate Weibull parameters A and C [17] which provide quite similar results. For instance the method of moment yields the estimation of the mean (μ) and the variance (σ^2) of Weibull distribution as a function of the Weibull parameters

$$\mu = A\Gamma(1/C + 1) \text{ and } \sigma^2 = A^2(\Gamma(2/C + 1) - \Gamma^2(1/C + 1)) \quad (7)$$

Using the above equations the Weibull parameters are determined as:

$$C = (\sigma/\mu)^{-1.086} \text{ and } A = \mu/\Gamma(1/C + 1)$$

The Weibull parameters are estimated at each grid cell and from the available time series. Spatial distribution of the scale parameter A is very similar to that of mean wind speed (not shown). Its values are mainly between 7.4m/s and 9m/s. The lowest values are located near coasts, while the highest are off coast and along English Channel. Spatial distribution of sharp parameter C exhibits more variability. Indeed, the highest values, about of 2.6, are mostly found in north zone related to narrower wind speed distributions, while the lowest of 2.2 are depicted in south of Brittany region where dominant peak is not well defined as shown in Figure 6.

To assess the accuracy of the Weibull fitting method, the mean and standard deviation of the empirical distribution (determined from observations) is compared to those estimated from the predicted distribution (eq. 4). Comparisons are performed for each grid cell using the Student's t-test. The main results (not shown) indicate that the empirical and predicted statistical means are comparable at the 95% confident level. Similar results are found for standard deviations comparisons.

The Weibull pdf also provides an estimation of the most probable wind speed (eq (7)) and the wind speed generating maximum energy (eq (8)):

$$W_{mp} = A\left(1 - \frac{1}{C}\right)^{\frac{1}{C}} \quad (7)$$

$$W_{\max} = A\left(1 + \frac{2}{C}\right)^{\frac{1}{C}} \quad (8)$$

The analysis of W_{mp} (eq. 7) and W_{max} (eq. 8), calculated for each year at each grid cell, indicates that both have significant spatial and temporal variabilities. In the north, minimum nearshore and offshore values of W_{mp} are about 5.5m/s and 7.5m/s, respectively. In the south, except at some specific locations, minimum values do not exceed 5.5m/s. W_{mp} maximum values fall within 10m/s and 11.5m/s in the north, and within 7m/s and 10m/s in the south.

The minimum values of W_{max} mostly range between 9m/s and 11m/s moving from nearshore to offshore. A large variation is seen south of Brittany where W_{max} minimum and maximum values are about 9.5m/s and 16m/s, respectively. The latter is associated with a storm which occurred on December, 26th 1999.No significant trend for the period 1999 – 2012 is found for either W_{mp} or W_{max}.

5.2. Height Issue

Scatterometer retrievals are available at 10m height as equivalent neutral winds (ENWs). The overall difference between ENW and "real" (including stratification impact) winds is about 0.20m/s. Better determination and characterization of wind energy estimated from scatterometer observations requires calculations at hub height. The latter generally range between 50m and 100m above the surface of the water. Therefore, the local shear component is required to accurately estimate the winds at the height of the hub from the 10m ENW scatterometer winds.

In the atmospheric surface boundary layer (SBL), similarity theory yields the logarithmic wind speed profile at height z (e.g. [13]):

$$W(z) = \frac{W}{k}\left(\ln\left(\frac{z}{z_0}\right) - \Psi\left(\frac{z}{L}\right)\right) \quad (9)$$

Where W_* is the friction velocity, k the von Kármán constant (generally taken to be 0.4), z_0 is the aerodynamic roughness length and the stability, Ψ, is a function of z/L, where L is known as the Monin-Obukhov lengthscale. For a neutral boundary layer $\Psi(\frac{z}{L}=1)=0$, the wind profile is :

$$W(z)=\frac{W}{k}\ln(\frac{z}{z_0}) \qquad (10)$$

The calculation of W(z) from (eq. 9) or from (eq. 10) is not straightforward and requires an iterative procedure (e.g. [13]). Furthermore, in addition to the 10m scatterometer winds, bulk variables such as sea surface temperature (SST), air temperature (AT) and relative humidity (RH) are also needed. These are obtained from the National Centers for Environmental Prediction (NCEP) Climate Forecast System Reanalysis (CFSR) [18]. They are available over global ocean with a spatial resolution of about 38km. Only CFSR SST, AT and RH available at synoptic times 00h:00, 06h:00, 12h:00, and 18h:00 UTC are used in this study. They are interpolated in space and time over ASCAT and QuikSCAT swaths using a bilinear method.

In this study only the winds at a height of 100m are estimated using the COARE3.0 model [5].

5.3. Spatial and temporal Characteristics

In previous sections, we clearly showed that scatterometer retrievals are accurate sources of wind information and thus a valuable resource to characterize geographical and temporal patterns of offshore wind energy along the coasts of Brittany. The spatial distributions of wind power density E determined from (eq. 5) based on 10m winds are shown in Figure 7 for four seasons. As expected, the spatial distributions have similar patterns to those obtained for winds (Figure 5). The highest and lowest values match high and low wind conditions. In winter, 95% of E values fall within 550 W/m² and 850W/m², whereas in summer this range is drastically reduced to 190W/m² and 340W/m². The E values estimated at 100m height fall within 1200W/m² and 1900W/m² in winter and within 370W/m² and 650W/m² in summer. Seasonal variations are more pronounced in certain areas. For instance, there is a factor of 4.5 between winter and summer E values estimated over the "Côtes d'Armor" offshore region located north of Brittany. Similar results are obtained for E estimated at 100m height.

The above results are calculated from all available valid scatterometer winds. To provide practical estimations of wind power density E, calculations are usually only performed for 10m wind speeds ranging between a minimum of 4m/s, called the cut-in, and a maximum of 25m/s, called the cut-off. We assume that for winds lower than the cut-in, not enough energy is available from the wind to allow for power production. For winds exceeding cut-off, the turbines would be shut down for self-protection.

Discrete and modeled (eq. 6) wind distributions are used to determine the percentage of winds occurring between the cut-in and cut-off limits. Both methods provide very close results. They indicate that winds are expected to fall within these limits nearly 86% of time. However this percentage has significant spatial and temporal variability. For instance, in the winter it increases to 93%, and in the summer it decreases to 79%. The related spatial distribution indicates that at near-shore locations, the percentages are slightly lower than those estimated at regional scale. They account for approximately 85%, 80%, 70%, and 82% during winter, spring, summer, and fall, respectively.

To further assess the temporal variability of E estimated at near-shore grid cells (i.e. where the distance to the shore is less than 50km), inter-annual and intra-annual time series are calculated for the period January 2000 – December 2012. For the spatial variability of E (Figure 7), intra- and inter-annual series are calculated for two near-shore zones located north (north Brittany) and south of 48°N28’ (south Brittany). To minimize the impact of biases related to differences in sampling length and to local effects of atmosphere and ocean on winds and thus on wind power energy, the time series are normalized by long-term averages as follows:

$$E' = \frac{\overline{E_m}}{\overline{\overline{E}}} \text{ and } E'' = \frac{\overline{E_y}}{\overline{\overline{E}}} \quad (11)$$

E’ and E″ are intra-annual and inter annual E series.

$\overline{E_m}$ (m is month number) indicates monthly averaged E calculated for each calendar month of the study period.

$\overline{E_y}$ is yearly averaged E calculated for each year of the study period.

$\overline{E}$ is E mean value calculated from all selected data.

Time series of E’ (Figure 8a) and E″ (Figure 8b) are shown in red for north and blue for south Brittany**.**

In the two zones E’ shows strong seasonal variations. The highest E’ values are found during winter for both regions. More specifically, E’ maximum values are found in December in the south, while in the north, maximum values found in December and January are very close. Minimum values in the zones are mainly found in June. Winter and summer intra-annual values differ by a factor greater than 3. Although E’ estimated for north and south Brittany are similar, the maximum values occur with a shift of one month, in January and December, respectively.

The inter-annual variability (Figure 8b) indicates significant year to year variability. The impact of data sources on such variability is evident. Indeed, the lowest E″ estimates are found for the period 2010-2012 where wind retrievals are mainly from the ASCAT coastal retrievals

(ASCAT_coast). The latter include coastal wind information that would be lower than offshore winds. The highest E″ values are found for 2002 and 2007 in both northern and southern areas, whereas the lowest wind power energies occur in 2005 and 2011. Note that the low winds which occur in 2010 are mostly in the southern zone. As expected from equation (5), these extreme E″ values are related to wind conditions. For instance, in 2002 high winds exceeding 24m/s occurred in February. The number of days when retrieved winds exceeded 16m/s is 22. Low E″ values found during 2005 are mainly associated with low winds which occurred in November and December.

6. CONCLUSION

Precise and accurate wind speeds and directions with high space and temporal resolutions are required for marine renewable energy (MRE) investigations. It is quite common to use in-situ data provided by meteorological centres or by research organisations as wind references. Indeed, their operational maintenance regimes and their technical and scientific validations ensure their accuracy. Furthermore, they provide winds with high temporal resolution. However, their spatial distribution cannot meet the MRE requirements. In the present study, remotely-sensed data derived from ASCAT and QuikSCAT scatterometers are used to assess the spatial and temporal wind and power energy characteristics along the coasts of Brittany during the period spanning December 1999 through December 2012. Selecting only valid retrievals based upon data quality flags, the sampling lengths of wind observations at each grid cell of 0.125°×0.125° are within 500 (near coast cells) and 6000 (off coasts cells). Such sampling lengths exceed the requirements for wind observations as described by Barthelmie et al [19]. They concluded that 150 observations are needed to characterize the mean and the variance of wind speed.

The topic of this study is not the validation of scatterometer retrievals, however, several papers have investigated previously the accuracy of ASCAT and QuikSCAT wind speed and direction (e.g. [4]). This study shows that scatterometer winds are in good agreement with meteorological station data in this region. For near-shore stations, the correlation between in-situ and scatterometer wind speed exceeds 0.80, which indicates the coherency of the two observation methods.

The sampling length of the scatterometer observations and the comparisons of in-situ data and retrievals presented here show that remotely-sensed data can be used to accurately characterize the wind speed distributions and thus the associated wind power energy at regional scales. However, the main limitation of scatterometer data for wind and energy distribution studies is related to the radar sampling which depends on the satellite orbit characteristics. As both ASCAT and QuikSCAT data are mainly available in the morning and evening, the data may not adequately resolve the diurnal cycle. The impact of errors due to the scatterometer sampling schemes is investigated using comparisons between wind distribution parameters estimated for each station from all valid in-situ data and from in-situ data occurring close to scatterometer overpasses. The findings show that the sampling error has a small impact on the distribution results. In fact, the two estimations of the distribution parameters are comparable at a confidence level of 95%. The second main limitation of remotely-sensed winds is that the retrievals are given as equivalent neutral winds (ENW) at 10m height. No vertical wind profile is available from scatterometer measurements. To circumvent this limitation, the estimation of wind at hub height (50m - 100m) is performed using the COARE3.0 parameterization [5]. The required bulk variables are 10m winds from scatterometers, 10m air temperature, 10m specific air humidity, and sea surface temperature which were obtained from CFSR re-analyses.

The analysis methods summarized above enable the characterisations of winds and the related wind power around the coasts of Brittany coasts. The highest and lowest wind conditions are found over the north-west and south-east zones, respectively. For instance, the maximum values of the most probable wind speed are within 10m/s and 11.5m/s in the north, whereas in the south they are within 7m/s and 10m/s. Although the prevailing winds are westerly, wind directions exhibit high variability. Indeed, during winter season westerlies account only for 14% and 11% in north and south areas, respectively. For wind power evaluation purpose, the use of scatterometer winds indicate that on average 86% of data are within the cut-in and cut-off limits. However, this percentage has significant spatial and temporal variation. As expected, the wind power exhibits similar patterns to wind speed. For instance, the highest and lowest values are found in winter and summer, respectively. However, the seasonal variation is more pronounced at specific locations, such as Côtes d’Armor.

This study highlights the usefulness of the long time series of remotely-sensed winds for the evaluation and the analysis purposes of wind power off Brittany coasts. Further improvements are expected through the combination of scatterometer, in-situ, and regional numerical model data to investigate finer space and time wind scales and their impact on energy resource potential.

Acknowledgement

We are grateful to JPL, EumetSat, KNMI, Météo-France, Cersat/Ifremer for providing valuable remotely sensed and in-situ data used in this study. We thank Dr Jenny Hanafin for her very helpful comments on the manuscript.

References

[1] Sanchez R., P. Relvas, H. O. Pires, 2007: Comparisons of ocean scatterometer and anemometer winds off the southwestern Iberian Peninsula. Continental Shelf Research, Vol. 27, Issue 2, pp 155–175. doi:10.1016/j.csr.2006.09.007

[2] Pimenta F., W. Kempton, R. Garvine, 2008: Combining meteorological stations and satellite data to evaluate the offshore wind power resource of Southeastern Brazil, Renewable Energy, 33 , pp. 2375–2387. doi:10.1016/j.renene.2008.01.012

[3] Karagali, I., A. Peña,, M. Badger, C. B. Hasager, 2012: Wind characteristics in the North and Baltic Seas from the QuikSCAT satellite. Wind Energy. doi: 10.1002/we.1565

[4] Bentamy, A., S. A. Grodsky, J. A. Carton, D. Croizé-Fillon, and B. Chapron, 2012: Matching ASCAT and QuikSCAT winds, *J. Geoph. Res., 117,* C02011, doi:10.1029/2011JC007479.

[5] Portabella, M., A. Stoffelen, W. Lin, A. Turiel, A. Verhoef, J. Verspeek and J. Ballabrera-Poy, 2012: Rain Effects on ASCAT-Retrieved Winds: Toward an Improved Quality Control IEEE *Transactions on Geoscience and Remote Sensing*, **50**, 7, 2495- 2506, doi:10.1109/TGRS.2012.2185933.

[6] Fore A., B. Stiles, R. S. Dunbar, B. Williams, A. Chau, L. Ricciardulli, F. Wentz, T. Meissner and E. Rodridguez, 2011: Point-wise wind retrieval and ambiguity removal improvements for the QuikSCAT climatological data set. International Ocean Vector Wind Science Team Meeting Annapolis, Maryland, USA, 9-11 May 2011 (http://coaps.fsu.edu/scatterometry/meeting/past.php#2011)

[7] Ricciardulli L. and F. Wentz, 2011: Reprocessed QuikSCAT (V04) wind vectors with Ku-2011 geophysical model function. Remote Sensing Systems Technical Report 043011 (http://www.ssmi.com/qscat/qscat_Ku2011_tech_report.pdf)

[8] Bentamy, A., D. Croize-Fillon, and C. Perigaud , 2008: Characterization of ASCAT measurements based on buoy and QuikSCAT wind vector observations, *Ocean Sci.*, *4*, 265–274.

[9] Verspeek, J.; A. Stoffelen, M, Portabella, H. Bonekamp, C. Anderson, and J.F. Saldana (2010), Validation and Calibration of ASCAT Using CMOD5.n, *IEEE Transactions on Geoscience and Remote Sensing*, *48*, 386-395, doi: 10.1109/TGRS.2009.2027896

[10] Verhoef, A., M. Portabella and A. Stoffelen, High-resolution ASCAT scatterometer winds near the coast. IEEE Transactions on Geoscience and Remote Sensing, 2012, 50, 7, 2481-2487, doi:10.1109/TGRS.2011.2175001.

[11] Grodsky, S. A., V. N. Kudryavtsev, A. Bentamy, J. A. Carton, and B. Chapron , 2012: Does direct impact of SST on short wind waves matter for scatterometry?, *Geophys. Res. Lett., 39*, L12602, DOI: 10.1029/2012GL052091.

[12] Jet Propulsion Laboratory (JPL), 2006: QuikSCAT Science Data Product User's Manual Overview & Geophysical Data Products, ftp://podaac-ftp.jpl.nasa.gov/allData/quikscat/L2B/docs/QSUG_v3.pdf

[13] Fairall, C.W., E.F. Bradley, J.E. Hare, A.A. Grachev, and J.B. Edson (2003), *Bulk Parameterization of Air–Sea Fluxes: Updates and Verification for the COARE Algorithm*, J. Clim., *16*, 571–591.

[14] Crosby, D.S., L.C. Breaker,and W.H. Gemmill, 1993: A proposed definition for vector correlation in geophysics: theory and application. *Journal of Atmospheric and Oceanic Technology*, **10**, 355 - 367.

[15] Hsu S. A., 1981: Models for estimating offshore winds from onshore meteorological measurements, Boundary Layer Meterology, Volume 20, Issue 3, pp 341-351

[16] Justus C.G., Hargraves W.R., Yalcin A. , 1976: Nationwide assessment of potential output from windpowered generators. Journal of Applied Meteorology, Vol. 15, pp 673–678. doi:10.1175/1520-0450(1976)015<0673:NAOPOF>2.0.CO;2

[17] Pavia E.G., O'Brien J.J. (1986). *Weibull statistics of wind speed over the ocean*. J. Climate Appl. Meteor., 25, pp 1324–1332. doi:10.1175/1520-0450(1986)025<1324:WSOWSO>2.0.CO;2

[18] Saha S., and Coauthors, 2010: The NCEP Climate Forecast System Reanalysis. *Bull. Amer. Meteor. Soc.*, **91**, 1015–1057. doi: http://dx.doi.org/10.1175/2010BAMS3001.1

[19] Barthelmie R J, Pryor S., 2003: Can satellite sampling of offshore wind speeds realistically represent wind speed distributions? Journal of Applied Meteorology 42(1)

Tables

Table 1 : Meteorological station Id and coordinates.

WMO Id	Name	Latitude	Longitude
07207	Belle Ile	47°17'41" N	3°13'6" W
07107	Brignogan	48°40'35" N	4°19’52" W
07116	Ile de Batz	48°45'0" N	4°1’0" W
07203	Ile de Groix	47°39'8" N	3°30'8" W
03895	Jersey	49°12'35" N	2°11'39" W
07109	Lanvéoc	48°17'0" N	4°26'0" W
07100	Ouessant	48°28'24" N	5°3'25" W
07117	Ploumanac'h	48°49'33" N	3°28'23" W
07200	Penmarc'h	47°47'51" N	4°22'29" W
07103	Pointe du Raz	48°2'20" N	4°43'55" W
07216	Saint Nazaire	47°14'2" N	2°17'55" W

Table 2: Statistics of differences between meteorological station and scatterometer wind speeds during the 2008 – 2012 period. bs and ρ are symmetrical regression coefficient and correlation coefficient, respectively.

Station	Length	Bias	STD	bs	ρ
All	92170	-0.81	2.21	0.95	0.83
07207	16630	-1.06	1.59	1.05	0.86
07107	5206	-1.53	1.82	1.07	0.82
07116	1443	-0.54	2.44	0.84	0.76
07203	6919	-0.44	1.36	0.97	0.87
03895	18125	-1.68	1.76	1.12	0.84
07100	18471	0.07	1.66	0.93	0.89
07117	4631	-2.39	1.60	1.37	0.84
07200	9421	-0.61	1.80	0.91	0.84
07103	9251	0.49	2.07	0.78	0.86
07216	2071	-1.78	2.32	0.73	0.75

Table 3: Statistical parameters calculated for each station, for all data (top row) and for selected (within one hour of scatterometer overpasses) data (bottom row).

Station	Length	Mean	Median	STD	Skew	Kur	P_{10}	P_{90}	P_{95}
07207	37288	6.01	5.61	3.06	0.93	4.28	2.58	10.00	11.81
	8994	5.91	5.50	2.96	0.86	4.07	2.50	9.81	11.31
07107	35992	5.95	5.31	3.29	0.96	3.96	2.31	10.50	12.30

	4533	5.79	5.19	3.22	0.86	3.58	2.11	10.31	12.18
07116	7886	6.51	6.17	3.48	1.26	7.81	2.61	11.30	12.89
	768	6.41	5.93	3.67	2.05	14.45	2.61	10.81	12.31
07203	34184	6.63	6.19	3.25	0.76	3.74	2.89	11.00	12.61
	3246	6.59	6.19	3.28	0.74	3.71	2.69	10.89	12.61
03895	59638	5.79	5.67	2.67	0.86	5.07	2.58	9.25	10.81
	6461	5.90	5.67	2.79	0.78	3.95	2.58	9.78	10.81
07100	36009	7.47	7.00	3.62	0.69	3.43	3.11	12.33	14.11
	8699	7.38	6.89	3.53	0.69	3.62	3.11	12.19	13.69
07117	36914	5.15	4.64	2.66	0.88	3.77	2.11	8.75	10.31
	3664	5.03	4.69	2.49	0.83	4.03	2.11	8.31	9.53
07200	36406	6.37	5.61	3.65	1.01	3.95	2.39	11.50	13.50
	6522	6.24	5.50	3.53	1.06	4.24	2.50	11.11	13.00
07103	36096	7.60	7.00	4.19	0.80	3.56	2.61	13.36	15.40
	5145	7.47	6.89	4.10	0.83	3.86	2.61	13.00	14.89
07216	33951	5.89	5.11	3.56	1.38	5.77	2.11	10.80	12.89
	3274	5.89	5.00	3.81	1.48	5.95	2.11	11.19	13.39

Figure captions

- **Figure 1**: Sampling length of ASCAT and QuikSCAT valid retrievals occurring during the period : October 1999 – October 2012.
- **Figure 2** : Meteorological station locations shown as cross symbols
- **Figure 3**: Spatial correlation between meteorological station and scatterometer 10m wind speeds as a function of distance separating the two source locations..
- **Figure** 4: Comparisons of collocated meteorological station and scatterometer wind speeds. Figure4a illustrates the results obtained for all collocated data, while Figure4b is for the satellite data collocated with the station at Ouessant.
- **Figure 5**: Seasonal mean wind speed (in color) and wind direction (arrows) estimated from scatterometer retrievals during the period January 2000 – December 2012
- **Figure 6**: Wind roses derived from scatterometer retrievals during the period January 2000 – December 2012. Figure 6a and 6b indicate the results obtained from data occurring north of 40°N for winter and summer seasons, respectively. Figure 6c and 6d illustrate similar results for data occurring south of 48°N
- **Figure 7:** Seasonal mean wind power (in color) estimated from scatterometer retrieval distributions during the period January 2000 – December 2012
- **Figure 8**: Intra-annual (Figure 8a) and inter-annual (Figure 8b) of wind power estimated from scatterometer retrieval distributions during the period January 2000 – December 2012

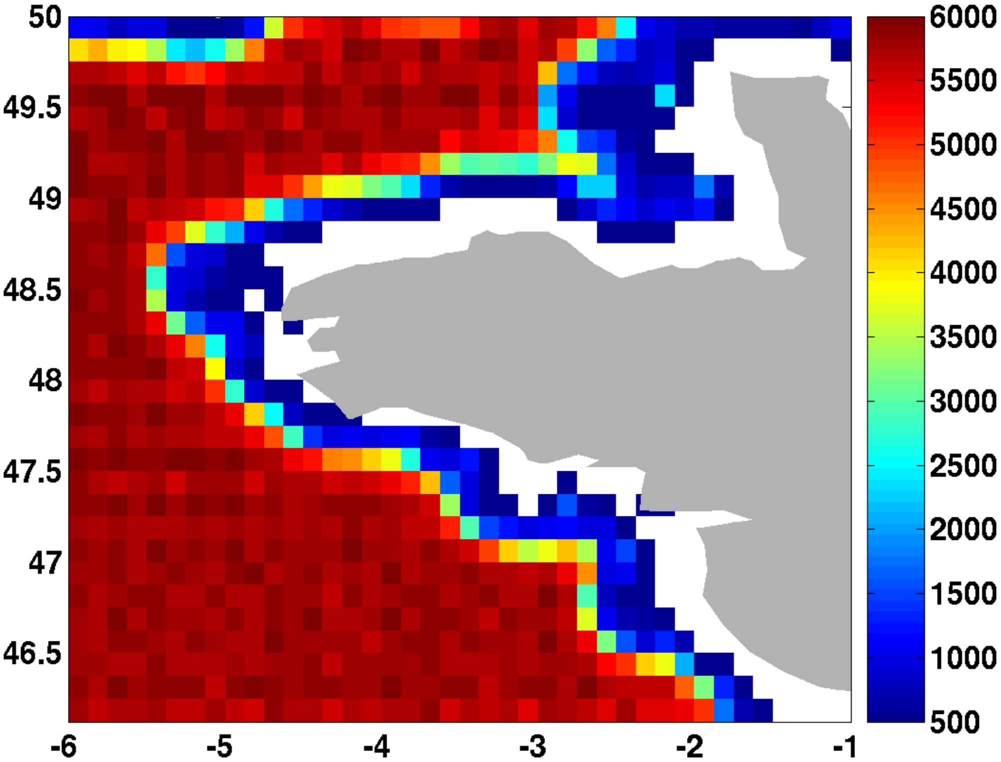

Figure 1: Sampling length of ASCAT and QuikSCAT valid retrievals occurring during the period : October 1999 – October 2012.

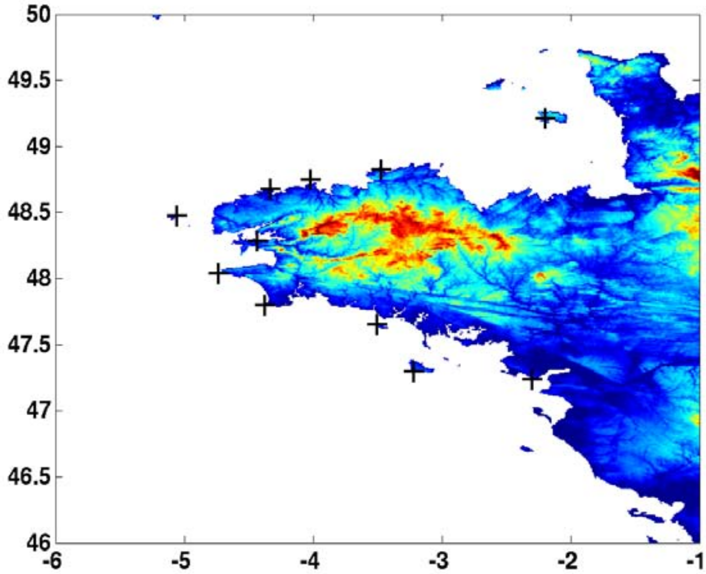

Figure 2 : Meteorological station locations shown as cross symbols

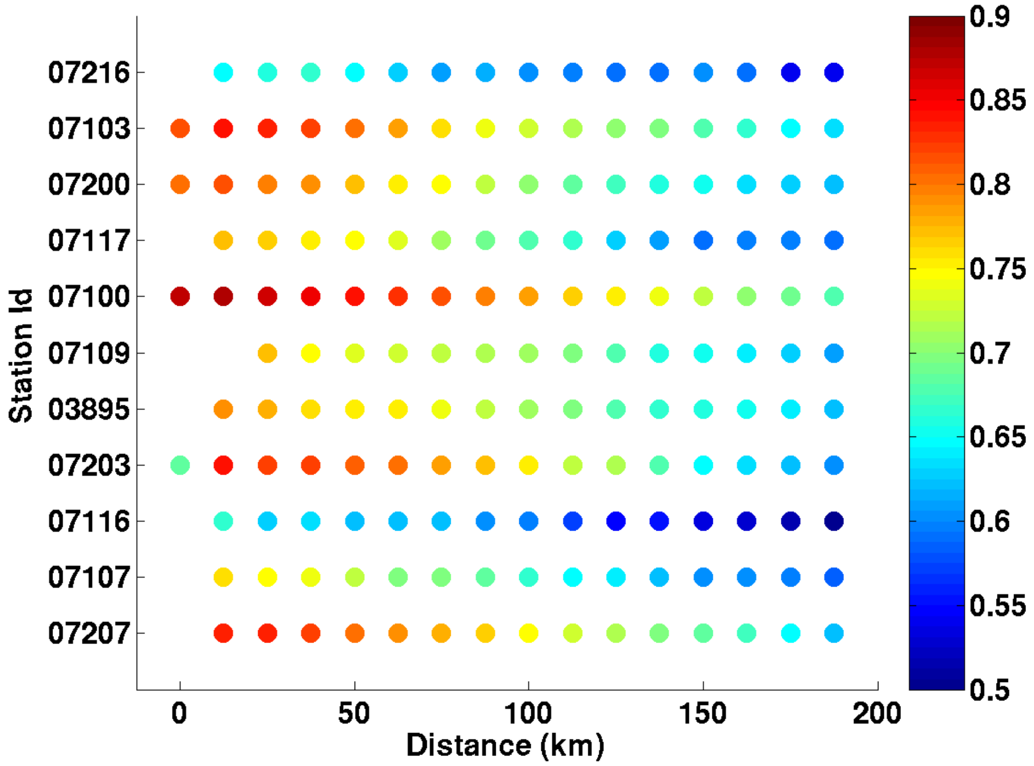

Figure 3: Spatial correlation between meteorological station and scatterometer 10m wind speeds as a function of distance separating the two source locations..

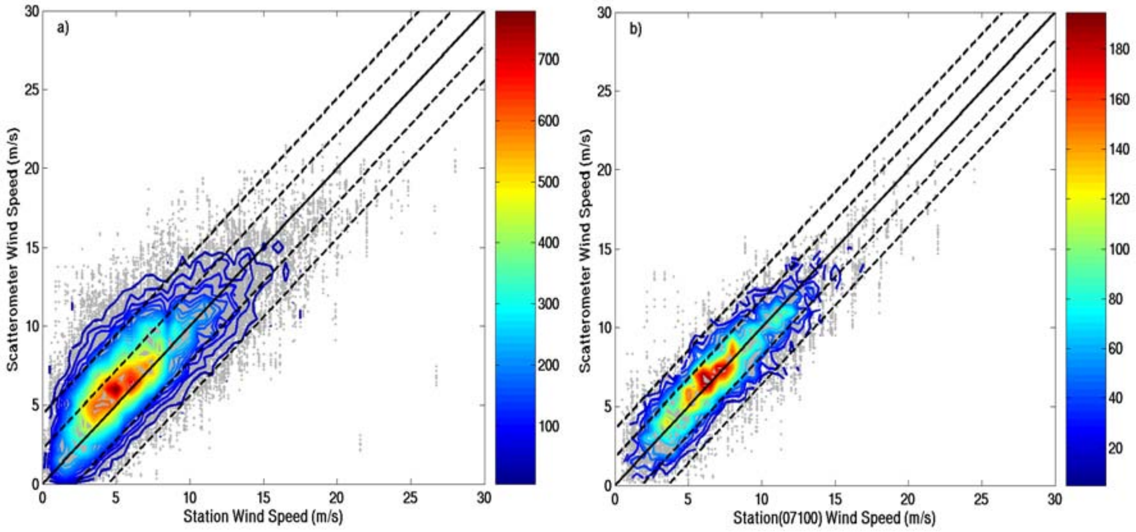

Figure 4: Comparisons of collocated meteorological station and scatterometer wind speeds. Figure4a illustrates the results obtained for all collocated data, while Figure4b is for Ouessant station and satellite collocated data

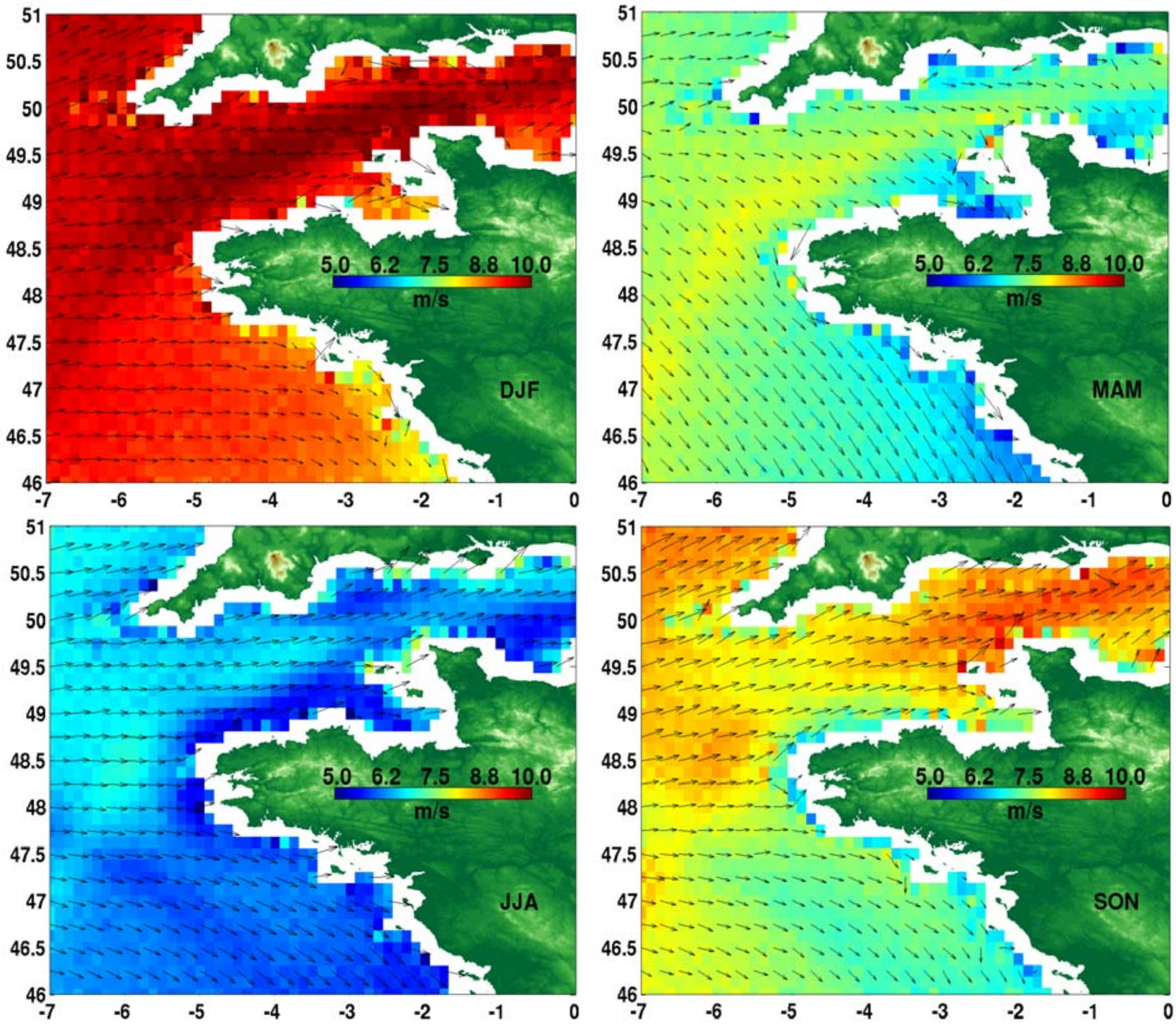

Figure 5: Seasonal mean wind speed (in color) and wind direction (arrows) estimated from scatterometer retrievals during the period January 2000 – December 2012

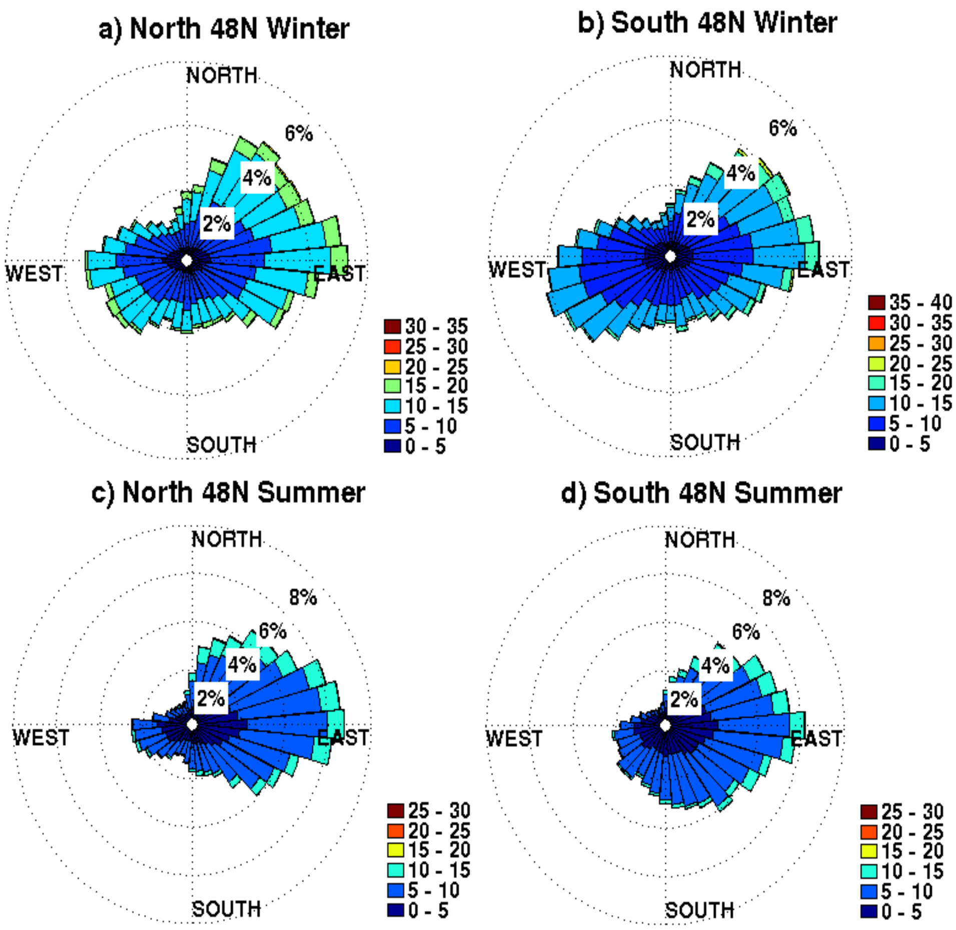

Figure 6: Wind roses derived from scatterometer retrievals during the period January 2000 – December 2012. Figure 6a and 6b indicate the results obtained from data occurring in north 40°N for winter and summer seasons, respectively. Figure 6c and 6d illustrate similar results for data occurring in south 48°N

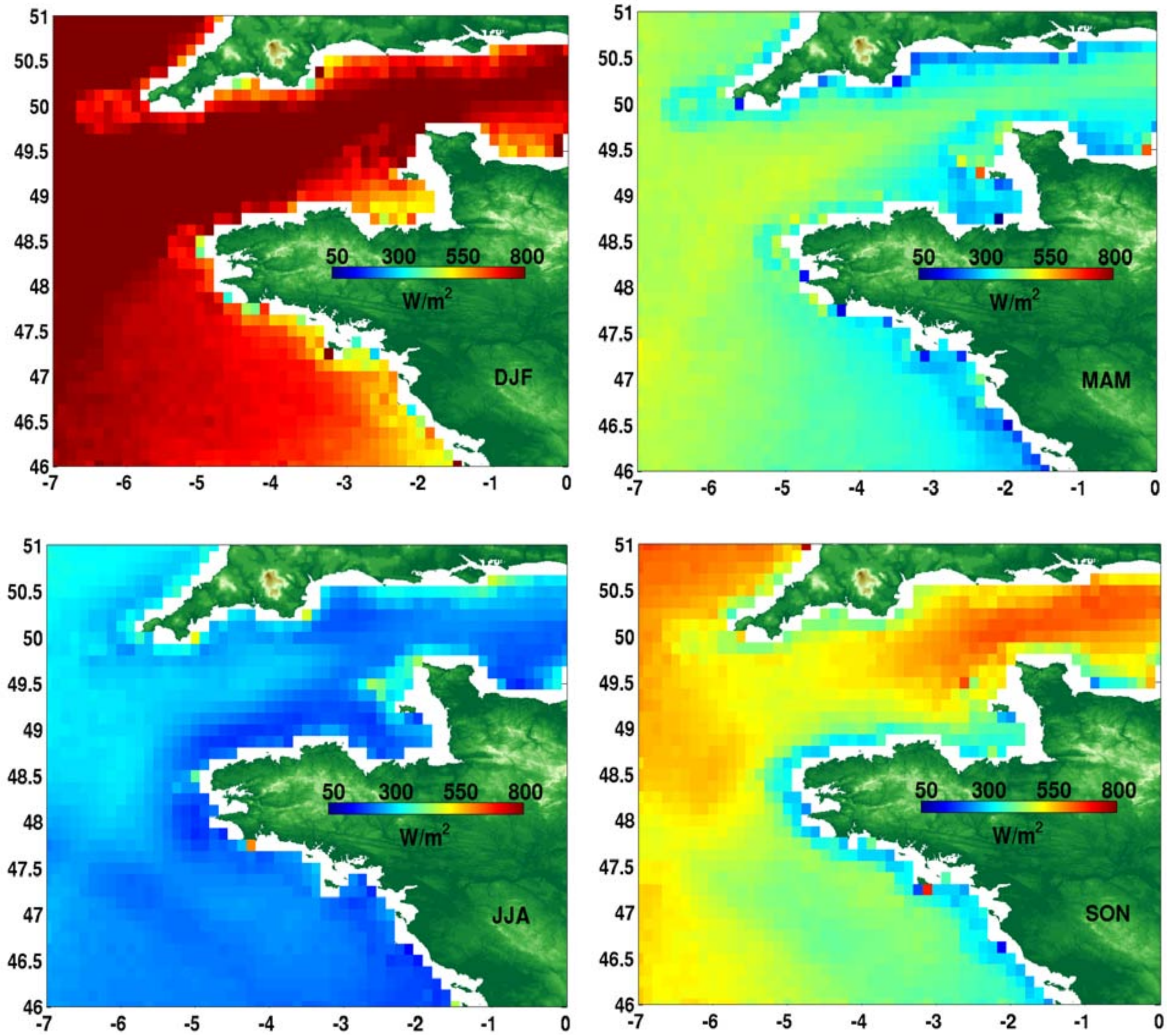

Figure 7: :Seasonal mean wind power (in color) estimated from scatterometer retrieval distributions during the period January 2000 – December 2012

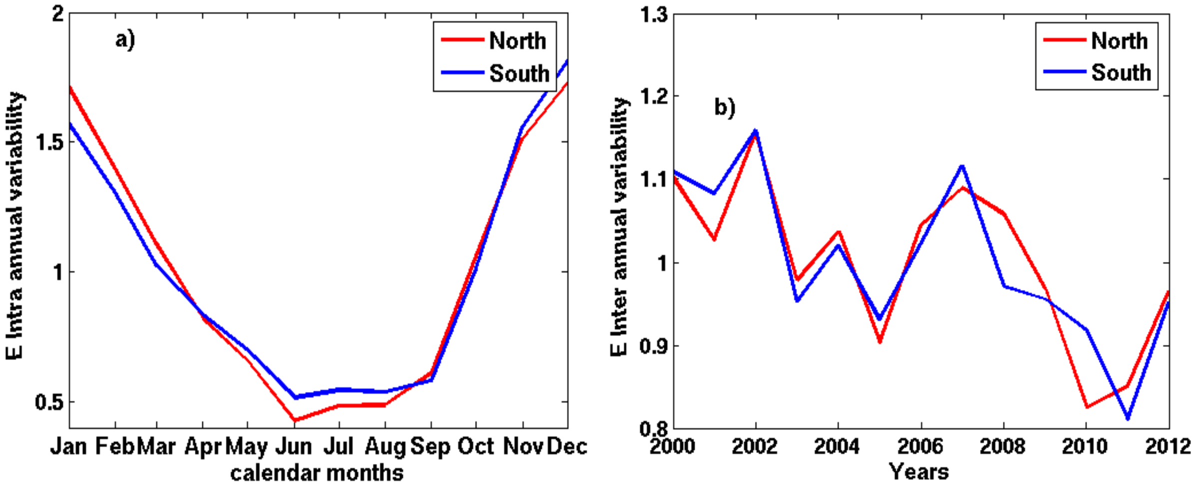

Figure 8: Intra-annual (Figure 8a) and inter-annual (Figure 8b) of wind power estimated from scatterometer retrieval distributions during the period January 2000 – December 2012